PCCP

PAPER

View Article Online
View Journal | View Issue

Cite this: *Phys. Chem. Chem. Phys.*, 2019, **21**, 8827

Si $1s^{-1}$, $2s^{-1}$ and $2p^{-1}$ lifetime broadening of SiX_4 (X = F, Cl, Br, CH_3) molecules: SiF_4 anomalous behaviour reassessed

Ralph Püttner, [a] Tatiana Marchenko,[bc] Renaud Guillemin,[bc] Loïc Journel, [bc] Gildas Goldsztejn,[b] Denis Céolin, [c] Osamu Takahashi, [d] Kiyoshi Ueda, [e] Alexsandre F. Lago, [f] Maria Novella Piancastelli [bg] and Marc Simon [bc]

Received 30th November 2018,
Accepted 29th March 2019

DOI: 10.1039/c8cp07369d

rsc.li/pccp

The Si $1s^{-1}$, Si $2s^{-1}$, and Si $2p^{-1}$ photoelectron spectra of the SiX_4 molecules with X = F, Cl, Br, CH_3 were measured. From these spectra the Si $1s^{-1}$ and Si $2s^{-1}$ lifetime broadenings were determined, revealing a significantly larger value for the Si $2s^{-1}$ core hole of SiF_4 than for the same core hole of the other molecules of the sequence. This finding is in line with the results of the Si $2p^{-1}$ core holes of a number of SiX_4 molecules, with an exceptionally large broadening for SiF_4. For the Si $2s^{-1}$ core hole of SiF_4 the difference to the other SiX_4 molecules can be explained in terms of Interatomic Coulomb Decay (ICD)-like processes. For the Si $2p^{-1}$ core hole of SiF_4 the estimated values for the sum of the Intraatomic Auger Electron Decay (IAED) and ICD-like processes are too small to explain the observed linewidth. However, the results of the given discussion render for SiF_4 significant contributions from Electron Transfer Mediated Decay (ETMD)-like processes at least plausible. On the grounds of our results, some more molecular systems in which similar processes can be observed are identified.

1 Introduction

Following ionization of a shallow inner-shell electron, the produced ions decay mainly by Auger processes, in which one electron from an upper level fills the core hole and another electron from the same or another shell is emitted. The lifetime for these processes is inversely proportional to the natural linewidth of the spectral features in the photoelectron spectrum. It is customary to describe the Auger spectra on the grounds of a one-center approximation, which includes only the Auger channels that induce two holes at the site where the primary vacancy is created, and neglects correlation effects (see *e.g.* ref. 1). This approximation is of particular interest when creating both holes in the valence shell since in this case the expected Auger rate depends on the electron density at the site of the initial core hole. If we consider a series of chemically related molecules, *e.g.* in our case the SiX_4 (X = F, Cl, Br, CH_3) sequence, we thus expect that the lifetime of the core hole is influenced by the nature of the substituents surrounding the central atom. In this framework, electronegative ligands supposedly withdraw outer electrons from the proximity of the core hole, rendering them less available to participate in Auger decay. Such ligands are, therefore, expected to lower the Auger rate and to increase the lifetime, thereby decreasing the natural linewidth of the spectral peaks. Therefore, in the above mentioned series, one expects the lifetime to be longer for the fluorinated compound, and to decrease accordingly for the other halogen-substituted molecules. However, it has been clearly shown that the SiF_4 compound shows a strong anomaly in the lifetime of the Si $2p^{-1}$ core hole.[2,3] In particular, the natural linewidth of the Si $2p^{-1}$ photoelectron line in this molecule is more than 5 times larger than the predicted value. At variance with that, the linewidths for $2p^{-1}$ photoelectron spectral features in SiH_4 and $SiCl_4$ are approximately as predicted.[3] The theoretical values for the core-ionized molecules were calculated by McColl and Larkins[1] using the above mentioned one-center model. Furthermore, in SiF_4 the Si $2p^{-1}$ Auger spectrum shows peculiarities that were explained in terms of electron correlation in ref. 4 and 5. While experimental results on the anomalous lifetime of the Si $2p^{-1}$ state in SiF_4 were consistently

[a] *Fachbereich Physik, Freie Universität Berlin, Arnimallee 14, D-14195 Berlin, Germany. E-mail: puettner@physik.fu-berlin.de; Tel: +49 30 838 56159*
[b] *Sorbonne Université, CNRS, Laboratoire de Chimie Physique-Matière et Rayonnement, LCPMR, F-75005 Paris Cedex 05, France*
[c] *Synchrotron SOLEIL, l'Orme des Merisiers, Saint-Aubin, BP 48, F-91192 Gif-sur-Yvette Cedex, France*
[d] *Department of Chemistry, Graduate School of Science, Hiroshima University, 1-3-1, Kagamiyama, Higashi-Hiroshima, 739-8526, Japan*
[e] *Institute of Multidisciplinary Research for Advanced Materials, Tohoku University, Sendai 980-8577, Japan*
[f] *Centro de Ciências Naturais e Humanas, Universidade Federal do ABC (UFABC), Rua Santa Adélia 166, 09210-170, Santo André-SP, Brazil*
[g] *Department of Physics and Astronomy, Uppsala University, Box 516, SE-751 20 Uppsala, Sweden*

reported by two different groups,[2,3] the explanation provided in the two studies was not the same. Namely, in ref. 3 the interpretation was that the valence electrons from the fluorine atoms play an important role in the Auger decay process. In ref. 3 approximate theoretical calculations were included, indicating that processes in which one of the participating electrons comes from the fluorine atoms are approximately as probable as those in which both electrons come from the silicon atom. They also draw an analogy with ICD (Interatomic Coulomb Decay) processes. In ref. 2 the interpretation relied on the so-called foreign image effect introduced by Cederbaum and coworkers.[4,5] In their original work[4] they defined foreign imaging as a spectral feature which gives a precise fingerprint of the atoms in the molecule that do not undergo core ionization. This is due to strong electron correlation in the final states resulting in pronounced two-hole localization at the ligand site. For SiF_4 this means that in the Si $2p^{-1}$ Auger spectra all dominant two-hole states are strongly localized on the fluorine atoms rather than on the silicon atoms. In fact, apart from the different models used, in both studies the role of fluorine atoms is underlined, due to the high electronegativity of the fluorine substituents and therefore to the high electron density on the neighboring atoms rather than on the central atom. In this framework, the high electronegativity plays a role which influences the lifetime of the core-ionized state in the opposite way as compared to the simple argument illustrated at the beginning: there is less electron density on the central atom, but the surrounding atoms are able to participate in the decay process. In the present work we report an extension of the previous measurements to the Si $2s^{-1}$ and Si $1s^{-1}$ core holes of the series SiX_4 (X = F, Cl, Br, CH_3). We have also repeated the Si $2p^{-1}$ measurements, which allow us to determine the experimental resolution precisely. In this way we are able to derive the natural linewidths of the Si $1s^{-1}$ and Si $2s^{-1}$ spectral lines with high accuracy. This was possible thanks to the state-of-the-art performance of the X-ray beam line, GALAXIES, located at the synchrotron SOLEIL, France, equipped with a high-resolution endstation dedicated to hard X-ray photoelectron spectroscopy (HAXPES) utilizing a hemispherical electron energy analyser designed for high electron kinetic energies. We show that the anomaly in the natural linewidth of the $2p^{-1}$ core-hole line in SiF_4 is not an isolated finding, but it is reflected also in the linewidths of the Si $2s^{-1}$ spectral features. For both core holes the lifetime broadening is about 50% larger than for $SiCl_4$.

In this publication we shall discuss the observed lifetime broadening of the Si $2s^{-1}$ and the Si $2p^{-1}$ core holes of SiF_4 in terms of non-local decay processes, namely ICD and Electron Transfer Mediated Decay (ETMD). Note that ICD and ETMD were originally defined[6,7] and extensively studied[8,9] for weakly bound systems like rare-gas clusters. In these systems the bond distances are large so that vacancies in the valence shell can be assigned to individual atoms. The presently studied molecules are, however, strongly bound so that the decay process involves delocalized molecular orbitals. Nevertheless, in this case an expansion of the molecular wavefunction into its atomic contributions allows us to assign electron density to individual atoms. Note that throughout this work we use the terms "ICD-like" as well as "ETMD-like" in order to emphasize this difference between weakly and strongly bound systems.

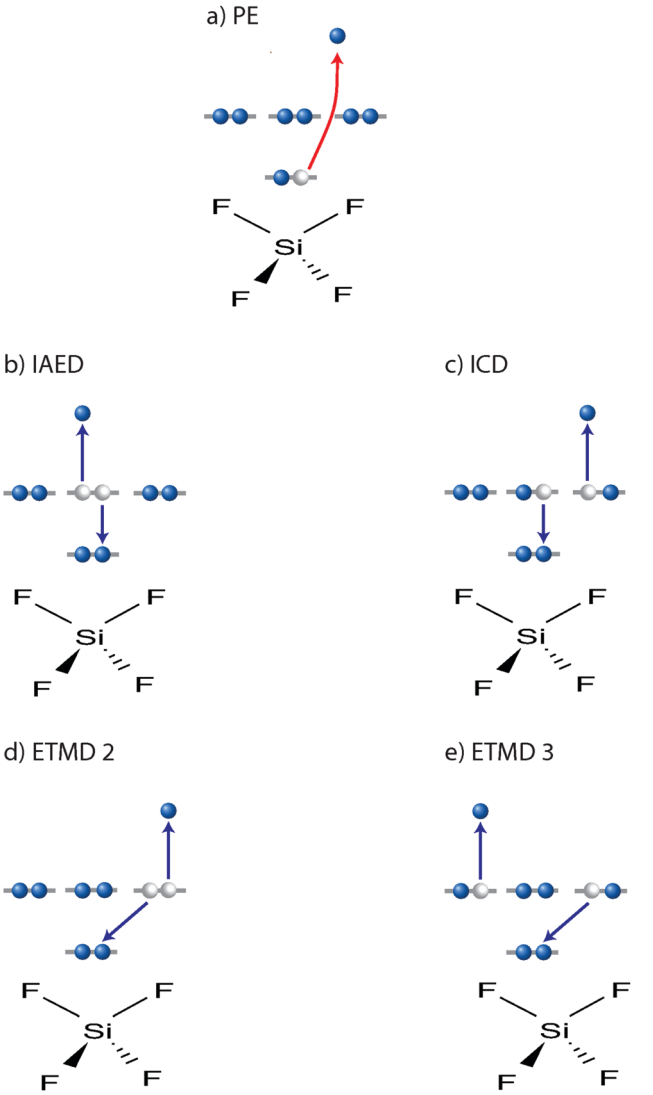

Fig. 1 Pictorial representation of the relevant processes using the SiF_4 molecule as an example. Presented are (a) the photoemission process (PE), (b) Intraatomic Auger Electron Decay (IAED), (c) Interatomic Coulomb Decay (ICD) and Electron Transfer Mediated Decay involving (d) 2 atoms (ETMD2) and (e) 3 atoms (ETMD3).

To illustrate the different non-radiative decay processes in a strongly bound system, one has to expand the molecular wavefunction into its atomic contributions. This allows one to attribute the Auger matrix elements including the core hole and valence orbitals to a specific decay process.[10] If the Auger decay occurs *via* two atomic valence orbitals of the Si atom the process can be assigned to Intraatomic Electron Decay (IAED), see Fig. 1(b). In the case that one atomic valence orbital of the Si and one of the F are involved it describes an "ICD-like" process, see Fig. 1(c), and in the case of two atomic valence orbitals of fluorine an "ETMD-like" process, see Fig. 1(d and e). Details of the involved Auger matrix elements will be discussed below around eqn (2).

In detail, the observed lifetime broadening of the Si $2s^{-1}$ core hole of SiF_4 can be explained with significant contributions of ICD-like processes using the model of Matthew and Komninos.[11] In contrast, this model does not provide a satisfactory explanation for the Si $2p^{-1}$ core-hole broadening of the same molecule, see Thomas *et al.*[3] However, a detailed comparison with the Xe $4d^{-1}$ decays of XeF_n (n = 2, 4, 6) molecules suggests distinct contributions of ETMD-like processes as an explanation of the observed lifetime broadening.[10] The results of the present studies predict significant ICD-like decay processes for a number of other fluorine-containing molecules like the S $2s^{-1}$ core hole of SF_6 as well as the P $2s^{-1}$ core hole of PF_3 and PF_5. Moreover, strong ETMD-like contributions are expected for the Ge $3d^{-1}$ core hole of GeF_4.

2 Experimental setup and data analysis

The measurements were performed at the SOLEIL synchrotron, France, on the GALAXIES beamline, with a endstation dedicated to HAXPES.[12] Linearly polarized light was provided by a U20 undulator and energy selected by a Si(111) double-crystal monochromator. Photoelectron spectra were collected with a SCIENTA EW4000 analyzer specifically designed for HAXPES, whose lens axis is set collinear to the X-ray polarization in a fixed geometry. The measurements of the SiX_4 spectra were performed at a photon energy of $h\nu$ = 2400 eV using an analyser pass energy of E_{pass} = 100 eV and a slit width of 300 μm. In this way a total experimental resolution of 270(10) meV was obtained. This value is derived from the Si $2p^{-1}$ photoelectron spectra of the different SiX_4 molecules, see below, and is also valid for the Si $1s^{-1}$ and $2s^{-1}$ spectra.

To obtain accurate binding energies from the photoelectron spectra, energy calibration was achieved in two steps. First, the kinetic-energy scale of the electron analyzer was calibrated by measuring Ar KMM and LMM Auger spectra. The Auger energies were calculated from binding energies of 3206.3(3) eV,[13] 248.63(1) eV,[14,15] and 45.14(1) eV[16] for the $1s^{-1}$, $2p_{3/2}{}^{-1}$, and $3p^{-2}(^1D_2)$ states of argon, respectively. Second, the photon energy was calibrated by measuring Ar $1s^{-1}$ and $2p_{3/2}{}^{-1}$ photoelectron spectra using the previously calibrated kinetic-energy scale. The described calibration procedure was repeated prior to the measurements of each individual molecule SiX_4 with X = F, Cl, Br, CH_3. Overall, the binding energies were determined with a systematic uncertainty of 0.4 eV. This value is mostly due to the uncertainty of 0.3 eV for the Ar $1s^{-1}$ binding energy. However, since the different SiX_4 spectra are calibrated in the same way with very similar calibration results, the relative values for the different molecules are expected to be accurate within 0.1 eV.

3 Results and discussion

Fig. 2 shows the Si $1s^{-1}$, Si $2s^{-1}$, and Si $2p^{-1}$ photoelectron spectra of the studied SiX_4 (X = F, Cl, Br, CH_3) molecules. From previous studies[2,3] it is known that the Si $2p^{-1}$ photoelectron spectra show vibrational progressions, partially even with significant hot-band contributions.[2,17] In the present case the vibrational progressions are masked because of the lower resolution due to the high photon energy. Similar vibrational progressions are also expected in the Si $1s^{-1}$ and the Si $2s^{-1}$ photoelectron spectra since different core holes should influence the valence shells of the molecules likewise and lead to similar molecular geometries. In the latter two cases, however, the natural linewidths alone are large enough to mask the vibrational progressions.

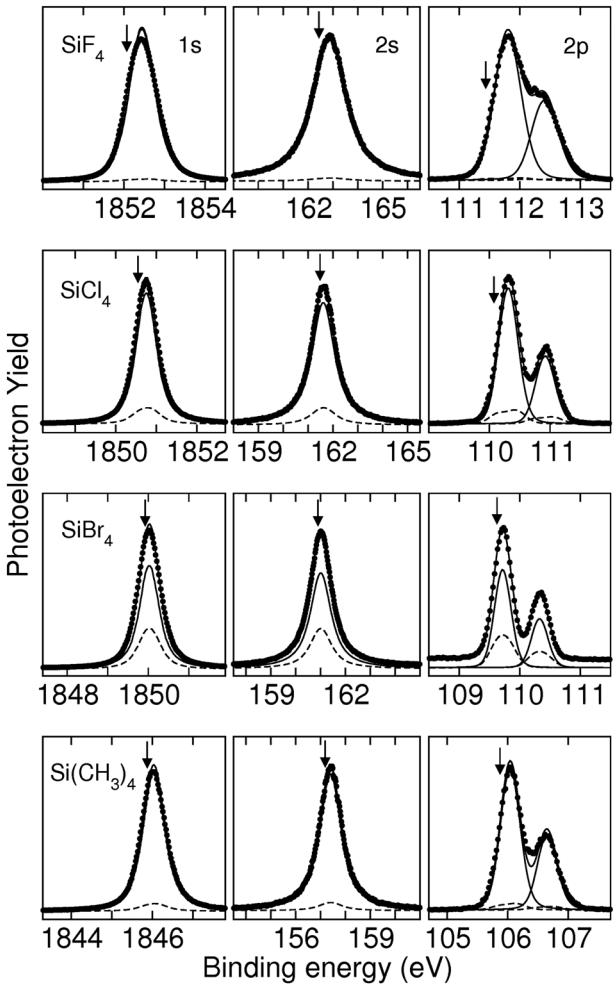

Fig. 2 The Si $1s^{-1}$, Si $2s^{-1}$, and Si $2p^{-1}$ photoelectron spectra of the molecules SiX_4 (X = F, Cl, Br, CH_3) recorded using a photon energy of $h\nu$ = 2400 eV. The solid line through the data points represents the fit results and the solid (dashed) subspectra indicate the contributions of the transitions starting from the vibrational ground state v'' = 0 (the higher vibrational substates $v'' \geq 1$) of the electronic ground state. The vertical arrows indicate the energy position of the v'' = 0 → v' = 0 transitions as derived from the fit approach.

3.1 The fit procedure

To extract the Si $1s^{-1}$ and Si $2s^{-1}$ lifetime broadenings as well as the binding energies of the vibration-free v'' = 0 → v' = 0 transitions the spectra were subject to a Franck–Condon fit analysis. Note that within this publication prime and double

prime indicate quantities related to the core-ionized and the ground state, respectively.

In the Franck–Condon fit analysis the vibrational progressions are calculated based on the Franck–Condon parameters, namely the equilibrium distance R_e, the vibrational energy $\hbar\omega_e$, and the anharmonicity $x\hbar\omega_e$ of the ground and the core-ionized state. In addition, since previous studies have shown that for some of the studied molecules hot bands play a significant role,[2,17] the thermal populations of higher vibrational substates are taken into account by assuming a temperature of 300 K. For details of the Franck–Condon analysis see ref. 2 and 18.

In the first step of the fit analysis, the Si $2p^{-1}$ spectra were fitted using the lifetime broadenings as well as the Franck–Condon parameters derived from the higher Rydberg states[2] to calculate the vibrational progressions. For SiF_4 and $SiCl_4$ the calculated vibrational progressions can be compared with Si $2p^{-1}$ ionized states from high-resolution photoelectron spectroscopy[3] revealing a good agreement. From these fits, the total experimental broadening, *i.e.* photon bandwidth, detector resolution, and Doppler broadening, was derived to amount to $\Delta E = 270(10)$ meV.

In the second step, this experimental broadening and the vibrational progressions of the Si $2p^{-1}$ states were used to fit the Si $1s^{-1}$ and Si $2s^{-1}$ photoelectron spectra. The results of the fit analyses are presented by the solid lines through the data points. The solid subspectrum indicates the transitions starting from the vibrational ground state of the electronic ground state, while the dashed subspectra represent the contributions of the "hot bands", *i.e.* from thermally populated vibrational levels of the electronic ground state. These "hot band" contributions are obviously small for SiF_4 and $Si(CH_3)_4$, but not negligible for $SiCl_4$ and $SiBr_4$.

The obtained binding energies for the $\nu'' = 0 \rightarrow \nu' = 0$ transitions are indicated in Fig. 2 with vertical arrows and summarized in Table 1. Obviously the $\nu'' = 0 \rightarrow \nu' = 0$ transitions are significantly below the centroids of the peaks. The error bars are derived by varying slightly the vibrational progressions in order to take into account some small differences in the geometry upon the creation of different core holes. For this purpose the vibrational energies $\hbar\omega'$ and the equilibrium distances R_e' of the core-ionized state are varied in the Franck–Condon analysis by 10% of the differences for $\Delta\omega = \omega' - \omega''$ and $\Delta R_e = R_e' - R_e''$.

3.2 The lifetime broadenings

In Table 2 the Si $1s^{-1}$ and Si $2s^{-1}$ lifetime broadenings obtained from the fit result are summarized. The error bars are derived in the same way as those for the binding energies. For comparison, literature values for the Si $2p^{-1}$ lifetime broadenings are also given. The Si $1s^{-1}$ lifetime broadenings are rather similar for the different molecules and amount to between 380 meV and 450 meV. However, for the Si 1s ionized states we want to point out that the fit result for SiF_4 is in the region of the peak maximum slightly worse than for all the other studied molecules. This minor mismatch might be due to slight saturation effects so that the lifetime broadening of SiF_4 may contain a systematic error towards larger values. Despite this possible systematic error all values are in reasonable agreement with the Si 1s lifetime broadening of 0.48 eV calculated for atomic silicon by Krause and Oliver.[19] The obtained values also fit to the experimental values of the sequence O $1s^{-1}$ ($\cong$170 meV),[20,21] Ne $1s^{-1}$ (250 meV),[20] and Ar $1s^{-1}$ (655 meV).[12] The experimental values for neon and argon are also reasonably well reproduced by the calculations of Krause and Oliver.[19] The discussed values clearly show that the presented fit approach results in reasonable values for the lifetime broadenings, although they are masked by vibrational progressions.

The Si $2s^{-1}$ lifetime broadenings for $SiCl_4$, $SiBr_4$, and $Si(CH_3)_4$ are between 900 meV and 950 meV and agree quite well with the theoretical value of 1.03 eV calculated for atomic silicon.[19] Contrary to this, the Si $2s^{-1}$ lifetime broadening for SiF_4 is 1438(25) meV, and so is significantly larger. This larger value can also be seen directly from the full widths of the different Si $2s^{-1}$ peaks, see Fig. 2, and it is consistent with the results of the Si $2p^{-1}$ threshold. The experimental results of Püttner *et al.*[2] and Thomas *et al.*[3] clearly showed that the Si 2p lifetime broadening of SiF_4 is much larger than the values for $SiCl_4$ and $SiBr_4$, contrary to the theoretical expectations.[1]

We notice that the anomaly is stronger at the Si $2p^{-1}$ threshold, where the linewidth value for the fluorinated compound is five times higher than the calculated value;[3] it is still quite high for the Si $2s^{-1}$ threshold, although less so, and it is

Table 1 The binding energies E_B for $\nu'' = 0 \rightarrow \nu' = 0$ transitions of the Si $1s^{-1}$, Si $2s^{-1}$, and Si $2p^{-1}$ core-ionized states of the different SiX_4 molecules. The values for the Si $1s^{-1}$ and Si $2s^{-1}$ states are derived from the Franck–Condon fit analysis while those for the Si $2p^{-1}$ states are taken from ref. 2 and used to reassess the calibration procedure. The numbers in parentheses represent the error bars on the last digit(s) as derived from the fit, see text. The absolute binding energies are additionally subject to an error of 0.3 eV due to the calibration of the energy scale while the relative values for the different molecules are accurate within 0.1 eV

	E_B (eV)		
	Si $1s^{-1}$	Si $2s^{-1}$	Si $2p^{-1}$ (ref. 2)
SiF_4	1852.08(5)	162.50(5)	111.45
$SiCl_4$	1850.55(8)	161.51(5)	110.10
$SiBr_4$	1849.93(10)	160.93(10)	109.64
$Si(CH_3)_4$	1845.89(5)	157.25(6)	105.89

Table 2 The Si $1s^{-1}$ and Si $2s^{-1}$ lifetime broadenings of the different SiX_4 molecules. The numbers in parentheses represent the error bars on the last digit(s) as derived from the fit, see text. For comparison, experimental and theoretical Si $2p^{-1}$ lifetime broadenings obtained in the literature are also given

	Lifetime broadening (meV)				
			Si $2p^{-1}$		
	Si $1s^{-1}$	Si $2s^{-1}$	Exp.[2]	Exp.[3]	Theo.[1]
SiH_4			50(5)	38(3)	32
SiF_4	450(20)	1438(25)	85(10)	79(5)	14
$SiCl_4$	380(20)	957(25)	48(2)	54(6)	32
$SiBr_4$	410(20)	896(20)	39(6)		
$Si(CH_3)_4$	439(20)	926(20)	76(9)		37

presumably still there for the Si 1s threshold, although almost within the error bars. This trend clearly means that, whatever the reason for this behavior, it has more influence for the shallow core levels, and it almost disappears as a function of the depth of the core hole. We can confirm the argument that the fluorine atoms play a decisive role in the Auger decay, and namely that the charge distribution induced by the highly electronegative substituents drives the Auger decay in a rather unusual direction, which we can call inter-atomic rather than intra-atomic, which would be the ''usual'' way. In fact, our data support it on the grounds of the above mentioned trend in the strength of the effect, since the fluorine electrons are more available to fill the shallower Si $2p^{-1}$ hole than the more core-like Si $2s^{-1}$ and especially the Si $1s^{-1}$ deep-core orbitals. Both the ICD-like and the foreign-image description are consistent with the present observations.

A comparable effect has been observed for Xe $4d^{-1}$ lifetime broadening of the sequence XeF_n with n = 0, 2, 4, 6. In this sequence an increasing number of electronegative fluorine ligands results in a withdrawal of valence-electron density at the Xe site. Hence in the one-center approximation a decrease of the lifetime broadening is expected, contrary to the experimental results.[22] This observation has been explained theoretically by C. Buth *et al.*[10] with contributions of interatomic decay processes, which are introduced above and depicted for the case of SiF_4 in Fig. 1. In detail, they took into account four different processes. The first process is IAED which leads in the case of XeF_n molecules to two holes at the Xe site and the second process is ICD which results in one hole at the Xe site and one hole at a F atom. The last two processes are two-monomer electron-transfer mediated decay (ETMD2) and three-monomer electron-transfer mediated decay (ETMD3), which lead to two holes at the same or at two different F-atoms, respectively.

As discussed above, the Si $2p^{-1}$ Auger spectrum of SiF_4 can be explained with the so-called foreign imaging model. In this case the final states visible in the Auger spectrum lead on average to $\cong$85% F^{-2} or $F_1{}^{-1}$ $F_2{}^{-1}$ populations, to $\cong$15% Si^{-1} F^{-1} populations and to less than 1% Si^{-2} populations,[4] due to strong electron correlation. At this point we want to emphasize that *e.g.* a large F^{-2} population of the final states does not necessarily lead to strong ETMD2 decays since the various decay channels show significantly different transition probabilities with strongly decreasing values from IAED to ICD to ETMD; for a more detailed discussion see the text around eqn (3). Contrary to the observations for the Si $2p^{-1}$ core holes, the much larger width of the Si $2s^{-1}$ core holes is assumed to originate from much faster Si $2s^{-1} \rightarrow 2p^{-1}val^{-1}$ Coster–Kronig Auger transitions leading to at least one hole located at the Si site, *i.e.* in this case the ETMD-like channels will not occur. Nevertheless, both the Si $2s^{-1}$ and $2p^{-1}$ lifetime broadenings of SiF_4 are about 50 to 60% larger than for $SiCl_4$ and $SiBr_4$.

In order to shed light on the experimental findings we will first discuss the data in terms of ICD-like processes by using a model established by Matthew and Komninos,[11] which was already applied by Thomas *et al.* to explain the unusual Si $2p^{-1}$ linewidth in SiF_4.[3] After this we will relate the situation for SiF_4 to the investigation of the Xe $4d^{-1}$ lifetime width of the different XeF_n (n = 2, 4, 6) molecules of Buth *et al.*,[10] where ETMD2 and ETMD3 processes were found to be of relevance.

3.3 ICD-like contributions to the lifetime broadening

The model of Matthew and Komninos[11] was originally developed for the case of diatomic molecules AB with an initial core hole on A and describes the rate $\tau_{\text{inter-intra}}{}^{-1}$ for ICD-like decays, which lead to a lifetime broadening Γ_{ICD} of

$$\Gamma_{\text{ICD}} = \hbar\tau_{\text{inter-intra}}{}^{-1} = \hbar\frac{c^4\sigma_k^{\text{B}}\tau_{\text{rad,A}}{}^{-1}}{\omega_\gamma{}^4 R^6} \qquad (1)$$

with c being the speed of light, σ_k^{B} the cross section for photoionization of this electron by a (virtual) photon of energy ω_γ, $\tau_{\text{rad,A}}{}^{-1}$ the X-ray decay rate of the core hole at atom A, and R the internuclear distance. As already used by Thomas *et al.*[3] the actual photoionization cross section σ_k^{B} is multiplied by the number of equivalent ligand atoms B. Note the high sensitivity of Γ_{ICD} to the internuclear distance due to the R^{-6} dependency.

With this model the ICD-like $2s^{-1}$ and $2p^{-1}$ lifetime broadening Γ_{ICD} was calculated for a number of selected molecules. The contributions to $1s^{-1}$ core holes were not calculated since a large value for $\hbar\omega_\gamma = E_{\text{B}}(1s) - E_{\text{B}}(2p) \cong 1840$ eV (compare $\hbar\omega_\gamma$ = 51 eV for Si $2s^{-1}$ and $\hbar\omega_\gamma$ = 91.5 eV for Si $2p^{-1}$), in combination with the $1/\omega_\gamma{}^4$ dependence, leads to negligible contributions. In the calculations for the Si $2s^{-1}$ core hole only the X-ray transitions to the $2p^{-1}$ core hole are taken into account, but not to the valence shell. This approach is justified by three facts, namely the dominating decay rate, the much lower value for ω_γ, and, as a consequence, the higher value for the ionization cross section of valence orbitals as compared to that belonging to a photon originating from the $2s^{-1} \rightarrow 3p^{-1}$ transitions. The results are summarized in Table 3 showing interesting results. For the ICD-like contributions of the Si $2s^{-1}$ core hole the values 963 meV and 736 meV are found by using an equilibrium distance of 1.486 Å for the core-ionized state[2,23] and 1.554 Å for the ground state,[24] respectively. The latter value of 736 meV is based on the assumption that subsequent to Si 2s ionization the Si–F bond distance does not have time to relax due to the short core-hole lifetime. This value agrees well with the difference of the lifetime broadening of SiF_4 and $SiCl_4$ as well as $SiBr_4$, suggesting an ICD-like contribution of 500 to 600 meV. For $SiCl_4$ and $SiBr_4$ the ICD-like contribution to the lifetime broadening is much smaller and almost identical. Contrary to this, the ICD-like $2s^{-1}$ lifetime broadenings of PF_3, PF_5, and SF_6 are $\cong$300–550 meV, in the same range as the value for SiF_4.

From these values we can conclude that the model of Matthew and Komninos explains the difference between the Si $2s^{-1}$ lifetime width of SiF_4 and the other SiX_4 molecules well in terms of ICD-like processes. The high Γ_{ICD} contribution to the Si $2s^{-1}$ lifetime width of SiF_4 is due to the small energy difference between the Si $2s^{-1}$ and Si $2p^{-1}$ holes as well as the particularly short bond distances in this molecule. Moreover, the results

Table 3 The calculated intra–inter atomic Auger decay rates, Γ_{ICD}, for different molecules and core holes. Given are also the used transition energy $E = \hbar\omega_\gamma$, the cross section for photoionization of this electron by a (virtual) photon of energy $\hbar\omega_\gamma$, σ_ν^{B}, the interatomic distance, R, and the radiative decay rate of the respective core hole, $\tau_{\mathrm{rad,A}}{}^{-1}$

Molecule	Core hole	R (Å)	$E = \hbar\omega_\gamma$ (eV)	σ_ν^{B} (Mb)	$\tau_{\mathrm{rad,A}}{}^{-1}$ (10^{-7} a.u.)	Γ_{ICD} (meV)
SiF_4	2s	1.486[a]	51[g]	29.0[k]	5.84[l]	963
SiF_4	2s	1.554[b]	51[g]	29.0[k]	5.84[l]	736
SiF_4	2p	1.486[a]	91.5[h]	13.2[k]	1.65[m]	12
$SiCl_4$	2s	1.953[a]	51[g]	2.8[k]	5.84[l]	18
$SiCl_4$	2p	1.953[a]	91.5[h]	4.6[k]	1.65[m]	0.8
$SiBr_4$	2s	2.103[a]	51[g]	3.2[k]	5.84[l]	13
PF_3	2s	1.570[c]	58[i]	18.0[k]	6.85[l]	302
PF_5	2s	1.534/1.557[d]	58[i]	18.0/12.0[k,d]	6.85[l]	542
SF_6	2s	1.575[e]	64[i]	29.0[k]	7.95[l]	371
SF_6	2p	1.575[e,f]	140[j]	6.0[k]	4.10[m]	1.7

[a] Ref. 2. [b] Ground-state value from ref. 24. [c] Ground-state value from ref. 25. [d] In PF_5 there are 2 inequivalent bond distances with 3 (2) F atom bonds at shorter (longer) distances. Given are the ground state values from ref. 26. [e] Ground-state value from ref. 27. [f] Almost no vibrational excitations are visible in the S $2p^{-1}$ spectrum of ref. 28 indicating a minor change of the bond distance upon ionization. [g] From data in Table 1. [h] Ref. 29. [i] Ref. 30. [j] Estimated from data in ref. 29. [k] Estimated from data in ref. 31 and multiplied by the number of equivalent ligand atoms. [l] Ref. 32. [m] Ref. 33.

suggest that a similar effect can be observed for the P $2s^{-1}$ and S $2s^{-1}$ core holes of F-containing molecules.

In contrast to Γ_{ICD} for the Si $2s^{-1}$ core hole of SiF_4, the value for the Si $2p^{-1}$ core hole of the same molecule, as well as the value for the S $2p^{-1}$ core hole of SF_6, was determined only on the basis of the internuclear distance of the core-ionized state. This approach is justified by the fact that significant nuclear motion can occur during the core-hole lifetime as can be seen by the photoelectron spectra, which show a resolved vibrational progression; this indicates a core-hole lifetime comparable to the molecular oscillation period. Obviously, in the case of SF_6 the contribution to the lifetime is at 2 meV much smaller than in case of SiF_4 at 12 meV.

Contrary to the $2s^{-1}$ core hole of SiF_4, where the calculated Γ_{ICD} is comparable to the deviation from the other molecules and the value for the Si atom, for the $2p^{-1}$ core hole the predicted values are too small to explain the observations. Actually, the difference between the lifetime width calculated in the one-center approximation of 14 meV and the measured value of $\cong$85 meV is about 6 times larger than Γ_{ICD}. The difference between the averaged value of $SiCl_4$ and $SiBr_4$ of $\cong$43 meV and the value measured for SiF_4 is also by more than a factor of 3 larger than Γ_{ICD}. These findings suggest that in the case of the Si $2p^{-1}$ core hole in SiF_4 an ICD-like process is not sufficient to explain the experimentally observed lifetime.

Finally we shall shortly discuss the accuracy of the model established by Matthew and Komninos[11] since it assumes no overlap of the atomic wavefunctions of atoms A and B and is, therefore, strictly valid only for large internuclear distances. Averbukh *et al.*[34] showed for the Ne 2s ionization of a NeMg van der Waals cluster that the overlap of the initial hole and the valence orbital of the neighboring atom can lead to a significant increase of the ICD-contributions to the lifetime broadening. However, in the present cases we consider core holes instead of valence orbitals so that the overlap is expected to be rather small as discussed further below. In addition to this, the formation of a SiF_4 molecule leads to a migration of electronic charge from the Si atom to the F atoms. On the one hand this leads to a reduction of the radiative decay rate $\tau_{\mathrm{rad,A}}{}^{-1}$; here Thomas *et al.*[3] estimate a factor of 2 for SiF_4 based on a Mulliken population analysis. On the other hand an increased charge density at the fluorine site causes a slight increase of the photoionization cross section σ_ν^{B}. Consequently, the obtained ICD-like contributions have to be considered only as approximate values. However, we want to point out that we found for the case with the largest calculated ICD-like contribution, namely the Si $2s^{-1}$ core hole of SiF_4 with Γ_{ICD} = 736 meV, good agreement with the difference of 500–550 meV between the observed lifetime broadening and the expected IAED contribution. This suggests that the formula of Matthew and Komninos[11] provides for the present class of cases at least semi-quantitative results.

3.4 ETMD-like contributions to the lifetime broadening

As mentioned above, for a sequence of XeF_n molecules with n = 2, 4, 6, Buth *et al.*[10] showed that ETMD-like processes make a significant contribution to the Xe $4d^{-1}$ core-hole lifetime width. In the following we shall discuss this possibility for the Si $2p^{-1}$ core hole in the SiF_4 molecule. For this purpose, we shall first give a short summary of the arguments in the work of Buth *et al*. In the case of the XeF_n molecules the Auger spectrum can be explained with the so-called foreign–imaging picture, *i.e.* a population analysis described in detail in ref. 35 shows that the two-hole final states have mainly a F^{-2} or $F_1{}^{-1}F_2{}^{-1}$ configuration (79.7% for XeF_6), *i.e.* the two holes are located either at one or two different fluorine atoms. To a smaller extent they have $Xe^{-1}F^{-1}$ character (19.1% for XeF_6), *i.e.* one hole at the xenon atom and one hole at the fluorine atom. Finally, the Xe^{-2} character of the final states is almost negligible (1.2% for XeF_6) and very uniformly distributed over the entire spectrum, so that the spectrum cannot be explained with two holes located at the xenon atom.

As we shall discuss in the following, this has consequences for the Coulomb matrix elements, which are necessary to calculate the Auger spectra and the lifetime width. The Coulomb matrix element is given by

$$J = \int v_i^*(r_1)k^*(r_2)\frac{1}{|r_1 - r_2|}v_{\mathrm{f}}(r_1)v_{\mathrm{f}'}(r_2)\mathrm{d}^3r_1\mathrm{d}^3r_2 \qquad (2)$$

with ν_i being the initial vacancy, k the continuum wave function and ν_f and $\nu_{f'}$ the two vacancies in the final state. For molecular Auger decay involving the valence shell ν_f and ν_f' are normally considered as molecular orbitals. However, to separate the Auger decay into the four different contributions presented in Fig. 1 we consider ν_f and ν_f' as atomic orbitals obtained by an expansion of the molecular orbitals into their atomic contributions. Using this approach, in the one-center approximation only those matrix elements are taken into account where ν_f and ν_f' are located at the core-hole atom and one refers to IAED processes. However, already Siegbahn *et al.*[36] pointed out that this one-center approximation is only a good approximation if the molecular orbital coefficients at the other atoms are not too large. Obviously the results of the above described population analysis lead to a violation of the prerequisite for the one-center approximation. Because of this also Coulomb matrix elements with one or both of the vacancies ν_f and $\nu_{f'}$ located at a ligand atom have to be taken into account. If still one vacancy is located at the core-hole atom, the matrix element describes an ICD-like process. Finally, an ETMD-like process is described when both vacancies are located at ligand atoms.

The population analysis of the XeF_n molecules described above is performed with the ADC(2) method based on Green's function calculations. These calculations do not result in Auger rates for the decay of the core hole to the individual final states, but the obtained pole strengths are a measure of the Auger intensity. As shown by Buth *et al.*[10] the total lifetime width Γ is given by the sum of the partial contributions to the lifetime width caused by the different decays, *i.e.* Γ_{IAED}, Γ_{ICD}, Γ_{ETMD2}, and Γ_{ETMD3}, which are given by the product of the two-hole population factor Q_i (i = IAED, ICD, ETMD2 and ETMD3) for the Xe^{-2}, $Xe^{-1}F^{-1}$, F^{-2} and $F_1{}^{-1}F_2{}^{-1}$ character of the final states, respectively, and a transition strength $|T_i|^2$ for each process,[10] *i.e.*

$$\Gamma = \sum_i \Gamma_i = \sum_i Q_i |T_i|^2. \quad (3)$$

Here, $|T_i|^2$ represent the squares of the Coulomb matrix elements given in eqn (2) averaged over all final states of the respective decay channel. Buth *et al.* calculated $|T_{IAED}|^2 = 1.4 \times 10^{-2}$ eV, $|T_{ICD}|^2 = 1.9 \times 10^{-3}$ eV, and $|T_{ETMD2}|^2 = |T_{ETMD3}|^2 = 2.1 \times 10^{-4}$ eV and obtained with these values *e.g.* for XeF_6 $\Gamma_{IAED} = 0.07$ eV, $\Gamma_{ICD} = 0.15$ eV, $\Gamma_{ETMD2} = 0.01$ eV, and $\Gamma_{ETMD3} = 0.06$ eV, *i.e.* all channels contribute significantly to the total lifetime width.

Typical Auger spectra, like *e.g.* the Si $2p^{-1}$ spectra of $SiCl_4$[37] of SiH_4,[38,39] show only a small number of transitions to final states with large Si^{-2} population. In contrast to this, foreign-imaging spectra are due to strong electron correlation and show a large number of transitions to final states, which all show similar two-hole populations with $Q_{IAET} \ll Q_{ICD} \ll Q_{ETMD}$, see above. As already mentioned above, eqn (3) shows that such a foreign-imaging spectrum does not necessarily include ICD-like or ETMD-like decay processes since the values for $|T_{IAED}|^2$, $|T_{ICD}|^2$ and $|T_{ETMD}|^2$ with $|T_{IAED}|^2 \gg |T_{ICD}|^2 \gg |T_{ETMD}|^2$ have also to be taken into account and can lead to an overcompensation of the two-hole population. Actually it has been shown by calculations that in addition to the XeF_n molecules the Auger Si $2p^{-1}$ Auger spectrum of SiF_4,[4] the C $1s^{-1}$ Auger spectrum of CF_4, the B $1s^{-1}$ Auger spectrum of BF_3,[40] and the S $2p^{-1}$ Auger spectrum of SF_6[41] can be explained with foreign imaging. In all cases a population analysis showed that the two-hole final states visible in the spectra have mainly F^{-2} or $F_1{}^{-1}F_2{}^{-1}$ character, and to a much smaller extent $X^{-1}F^{-1}$, while the X^{-2} character of the final states is almost negligible. Nevertheless, beside SiF_4 no unusual large linewidths have been reported in the literature. This observation in combination with our analysis of ICD-like processes given above and ETMD-like processes discussed below strongly suggests that for all the mentioned molecules but SiF_4 the values for $|T_{ICD}|^2$ and $|T_{ETMD}|^2$ are negligible so that the corresponding processes show only small contributions to the lifetime broadening.

In the following we shall qualitatively discuss for SiF_4 the size of the transition strength $|T_{ETMD}|^2$ in order to estimate possible ETMD-like decay processes. As mentioned above, this process is described by a Coulomb matrix element with ν_f and $\nu_{f'}$ being located at F-atoms. To have a large $|T_{ETMD}|^2$ there has to be a large overlap between the initial core hole ν_i and ν_f as well as between the continuum wavefunction k and $\nu_{f'}$. Due to the overlap argument for the core hole ν_i and the valence orbital ν_f located at a fluorine atom the EDMT-like contributions decrease exponentially with the internuclear distance. This is due to the exponential decrease of atomic wavefunctions with large distances from the nucleus.

To study the first overlap, we shall first discuss the situation for the XeF_n (n = 2, 4, 6) molecules where for the Xe 4d core hole ETMD-like decays occur.[10] For this case Fig. 3(a) shows the Xe 4d ground-state wavefunction based on Slater-type orbital expansions.[44] As a measure for how deep this wavefunction penetrates the fluorine region of the molecule, the halves of the Xe–F bond distances are also indicated. For XeF_6 two different distances are given due to the C_{3v} symmetry resulting in two bond lengths with a multiplicity of three each.[45] As can be seen in the figure, the Xe 4d wavefunction penetrates for all three molecules the region of the fluorine atoms. This effect increases with increasing n, *i.e.* it shows the same behavior as for Γ_{ETMD3} of the different XeF_n molecules. This observation suggests that the ETMD3-like decay channel is due to a considerable overlap of the Xe 4d core hole with the valence electrons located around the fluorine atoms.

In Fig. 3(b) the Si 2p (red line) radial wavefunction based on the coefficients given by ref. 44 is shown, together with the half of the SiX_4 bond distance (X = F, Cl, Br). The figure clearly shows that the Si 2p wavefunction penetrates in the case of SiF_4 the region of the fluorine ligand. Contrary to this, for $SiCl_4$ and $SiBr_4$ this penetration of the region of the ligand is much smaller. In a direct comparison of the XeF_n molecules and the SiF_4 molecule it can be seen that the respective Xe 4d and Si 2p wavefunctions penetrate the region of the fluorine ligand. In addition, due to the much shorter bond distance of SiF_4 the silicon region is more strongly penetrated by valence orbitals of the F-atom than the xenon region of the XeF_n orbitals.

Fig. 3(b) shows also the S 2p wavefunction as well as the half of the bond distance of SF_6 in the ground state, which is a good

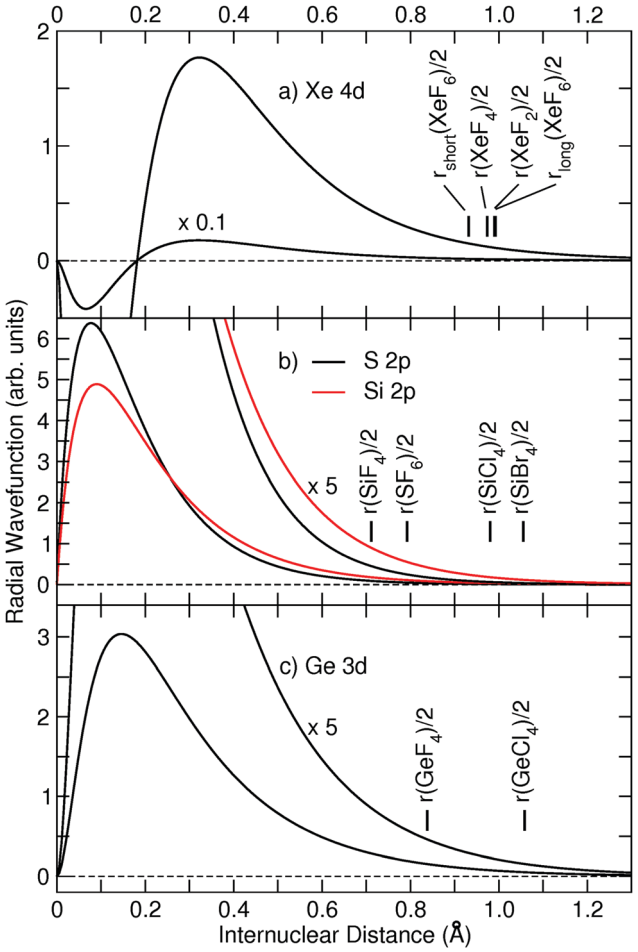

Fig. 3 (a) The radial part of the Xe 4d ground-state wavefunction. The halves of the different XeF_n bond distances are also indicated. (b) The radial part of the Si 2p and S 2p ground-state wavefunction together with the halves of the bond distances of SiF_4, $SiCl_4$, $SiBr_4$ and SF_6. (c) The radial part of the Ge 3d ground-state wavefunction together with the halves of the bond distances of GeF_4[42] and $GeCl_4$.[43]

approximation for the bond distance in the S $2p^{-1}$ ionized state, since the photoelectron spectrum shows only minor contributions of vibrational states.[28] The S 2p wavefunction is more contracted than the Si 2p wavefunction due to the higher charge of the sulfur nucleus. Contrary to this, the S–F bond distance is larger than the Si–F bond distance. As a result, the penetration of the S 2p wavefunction into the region of the fluorine atom is weaker. From these considerations the overlap between the core hole and a valence orbital at the fluorine site decreases along the sequence SiF_4, SF_6, $SiCl_4$ and $SiBr_4$.

In the next step we discuss the overlap of the second hole and the continuum wavefunction. As discussed above, ETMD is unlikely to occur in $SiCl_4$ and $SiBr_4$. Because of this we focus on fluorine as the ligand atom so that $\nu_{f'}$ can be considered similar for each molecule. As a result, we have to consider the continuum wavefunction alone. It is generally believed that the one-center approximation is valid only for higher Auger energies. With decreasing energies the wavelength of the continuum wavefunctions increases leading to a better overlap with the orbitals at the ligand atoms.[46] From this we conclude that the overlap of the second hole and the continuum wavefunction favors ETMD-like processes in the case of small Auger energies. Concerning this argument XeF_n and SiF_4 are the most likely candidates for ETMD-like processes since the average Auger energies increase along the sequence XeF_n,[10] SiF_4,[4] SF_6,[41] BF_3,[40] and CF_4[40] of molecules with Auger spectra that have to be explained with the foreign-imagine picture. Note that the higher Auger energy in SiF_4 as compared to XeF_n is at least partially compensated by the shorter bond distances, which allow a shorter wavelength for the continuum wavefunction.

In our discussion on ETMD presented so far we considered only the overlap between the core hole and the first valence electron as well as the second core hole and the continuum wavefunction. These overlaps are identical for ETMD2 and ETMD3 if relaxation is neglected so that the main differences between ETMD2 and ETMD3 are due to different values for $1/|r_1 - r_2|$. From these quantities, r_1 is mainly located in the overlap region of the core hole and the first valence electron and r_2 in the overlap region of the second valence electron and the continuum wavefunction. Generally, r_1 and r_2 are closer together when both valence electrons are from the same F-atom (ETMD2) than from different F-atoms (ETMD3), *i.e.* ETMD2 should be favored. However, calculations for XeF_4 and XeF_6 show that the ETMD3/ETMD2 ratios are close to the statistical ratios for forming $F_1^{-1}F_2^{-1}$ and F^{-2} final states, namely 3 : 1 for XeF_4 and 5 : 1 for XeF_6.[10] This suggest a minor influence of the $1/|r_1 - r_2|$-term on the probabilities for ETMD2 and ETMD3.

Other possible molecules for ETMD-like decay processes are GeF_4 and to a smaller extent $GeCl_4$ since in these cases the Ge 3d wavefunction penetrates the region of the halide atoms (see Fig. 3c), and the Auger energies are expected to be very low. This assumption is supported by the fact that the experimentally observed linewidth of GeF_4 is at $\cong$310 meV larger than that for $GeCl_4$ ($\cong$270 meV);[47] the corresponding experiments are, however, performed with medium resolution so that contributions caused by vibrational progressions cannot completely be ruled out. It is also interesting to note that the reported 3d lifetime broadening of GeH_4 is at $\cong$190 meV[47] significantly larger than that of the isoelectronic molecule HBr, which can be described well in the one-center approximation.[48] For the latter molecule lifetime broadenings between 97 and 111 meV[49] are reported for the different spin–orbit and ligand-field splitting components. This observation is in contrast to the isoelectronic molecules SiH_4[2,3] and HCl,[21] where the latter one shows the larger lifetime broadenings. Finally, we want to point out that all reported Ge $3d^{-1}$ lifetimes of GeX_4 molecules are at $\cong$200–300 meV much larger than the value of 48 meV calculated for atomic germanium.[50] All these findings suggest that the Ge $3d^{-1}$ holes of GeX_4 molecules provide an interesting possibility to study the influence of low-electron Auger decays on the lifetime broadening in detail.

In the following we shall qualitatively discuss the possibility of ETMD-like processes in SiF_4. For this we discuss the overlap arguments resulting from eqn (2) by comparing them for XeF_n and SiF_4. In detail, the overlap of the core hole and the valence

vacancy probably favors SiF_4 due to the shorter bond distance. The overlap of the second valence orbital and the continuum wavefunction should increase with decreasing bond distance and with decreasing Auger energy. Here the situation is less clear since the bond-distance argument favors the SiF_4 molecule while the Auger-energy argument prefers the XeF_n molecules. For XeF_n significant ETMD-like contributions to the lifetime have been shown by Buth *et al.*[10] It is consequently reasonable to assume that significant ETMD-contributions occur also for SiF_4, in particular since the estimated IAED-like and ICD-like lifetimes are not suited to explain the experimentally observed lifetime. Using the estimated ratio $|T_{IAED}|^2 = 10\cdot|T_{ICD}|^2 = 100\cdot|T_{ETMD}|^2$, which is close to the values obtained by Buth *et al.* for XeF_n molecules,[10] and the two-hole population ratio of 0.01 : 0.15 : 0.85 for $Si^{-2} : Si^{-1}F^{-1} : F^{-2}$ in SiF_4[4] we obtain $\Gamma_{IAED} : \Gamma_{ICD} : \Gamma_{ETMD} \cong 1 : 1.5 : 1$, *i.e.* all three processes contribute on the same order of magnitude. This is in reasonable agreement with the values Γ_{IAED} = 14 meV calculated by McColl and Larkins using the one-center approximation[1] and Γ_{ICE} = 12 meV estimated by Thomas *et al.*[3] based on the model of Matthew and Komninos.[11] However, for a definitive statement extended theoretical studies are necessary.

To summarize, we want to present an illustrating example. For this we performed for two-hole SiF_4 and $SiCl_4$ a Löwdin population analysis based on restricted Hartree–Fock (RHF) calculations for the ground states of both molecules. For SiF_4 we obtained a fraction of 1.17% for Si^{-2}, 19.3% for $Si^{-1}F^{-1}$, and 79.5% for $F_1{}^{-1}F_2{}^{-1}$ plus F^{-2}, which is in reasonable agreement with more specific calculations resulting in 1%, 15%, and 85%, respectively.[4] For $SiCl_4$ we obtained a fraction of 1.85% for Si^{-2}, 23.5% for $Si^{-1}Cl^{-1}$, and 74.7% for $Cl_1{}^{-1}Cl_2{}^{-1}$ plus Cl^{-2}. The Si^{-2} contributions of $SiCl_4$ are by $\cong$60% larger than that of SiF_4 so that the assumption of a similar value of $|T_{IAED}|^2$ for both molecules results in a significant increase of the lifetime broadening based on intra-atomic electron decay, in reasonable agreement with calculations specified for the Si $2p^{-1}$ core hole[1] resulting in 14 meV for SiF_4 and 32 meV for $SiCl_4$. Contrary to this, the relative changes for the $Si^{-1}X^{-1}$ and the $X_1{}^{-1}X_2{}^{-1}$ plus X^{-2} fractions are much smaller. However, as discussed above we expect for $SiCl_4$ (as well as for $SiBr_4$) due to the larger Si–X bond distances much smaller values for $|T_{ICD}|^2$ and $|T_{ETMD}|^2$ so that ICD-like and ETMD-like processes are strongly suppressed, *i.e.* instead of three comparable contributions IAED becomes clearly dominant. In particular, a comparison of the ICD-like $2p^{-1}$ lifetime contributions in Table 3 indicates that $|T_{ICD}|^2$ for $SiCl_4$ is by a factor of 15 to 20 smaller than for SiF_4.

4 Summary and conclusion

The Si $1s^{-1}$, Si $2s^{-1}$, and Si $2p^{-1}$ photoelectron spectra of a series of SiX_4 (X = F, Cl, Br, CH_3) molecules were measured and subject to a Franck–Condon fit analysis taking into account the change of the geometry upon ionization. Using the known Si $2p^{-1}$ core-hole lifetime widths the experimental resolution was determined to be 270(10) meV. This allowed determining for these molecules the Si $1s^{-1}$ and Si $2s^{-1}$ lifetime widths and revealed an anomalous short lifetime for the Si $2s^{-1}$ core hole in SiF_4 compared to the other studied molecules. This finding is in agreement with the results for the Si $2p^{-1}$ core hole, with a significantly shorter lifetime for SiF_4 than for the other studied molecules.

For the $2s^{-1}$ core holes the differences in the lifetime broadening for SiF_4 and the other measured SiX_4 molecules can be explained well with the model of Matthew and Komninos,[11] which describes ICD-like processes. Consequently, we assign the lifetime for the SiX_4 (X = Cl, Br, CH_3) to IAED processes and the difference to SiF_4 to ICD-like processes. For a better understanding of this finding, complementary studies on the Si $2s^{-1}$ Auger spectra of the different SiX_4 molecules are necessary. To record such data coincidence measurements have to be performed since the Si $2s^{-1}$ Auger spectra energetically overlap with those of the Si $2p^{-1}$ Auger spectra. Moreover, the model of Matthew and Komninos also predicts significant ICD-like Auger decay for the S $2s^{-1}$ core hole of SF_6 and the P $2s^{-1}$ core holes of PF_3 and PF_5. These results suggest to perform studies similar to those presented in the present work for a number of sulfur and phosphorus containing molecules including SF_6, PF_3, and PF_5.

Finally, for the Si $2p^{-1}$ core hole of SiF_4 the estimated IAED and ICD-like contributions are too small to explain the difference in lifetime between this molecule and $SiCl_4$ as well as $SiBr_4$. We believe that this discrepancy can be explained by the occurrence of ETMD-like processes. Such processes are calculated to cause significant contributions to the lifetime broadening of XeF_n (n = 2, 4, 6) molecules. A detailed comparison of the XeF_n (n = 2, 4, 6) molecules and SiF_4 leads to the conclusion that the bond distances and the Si $2p^{-1}$ Auger energies are also in favor of such processes. As another possible candidate for ETMD-like processes the Ge $3d^{-1}$ core-hole decay of GeF_4 is identified. However, for more definitive answers sophisticated calculations are necessary, and may be the subject of further investigations.

Author contributions

R. P., M. N. P., and M. S. devised the research, R. P., T. M., R. G., G. G., D. C., A. F. L., M. N. P., and M. S. participated in conducting the experimental research, R. P. performed the data analysis, O. T. performed the theoretical calculations, R. P., M. N. P., and K. U. wrote the paper, R. P. and L. J. prepared the figures, and all authors discussed the results and commented on the manuscript.

Conflicts of interest

There are no conflicts to declare.

Acknowledgements

Experiments were performed on the GALAXIES beamline at the SOLEIL synchrotron, France (Project No. 20130917). We are grateful to the SOLEIL staff for the smooth operation of the facility. The work at the Freie Universität Berlin was supported by the Deutsche Forschungsgemeinschaft under project no. PU180/6-1.

OT and KU acknowledge the support by the Research Program of ''Dynamic Alliance for Open Innovation Bridging Human, Environment and Materials'' in ''Network Joint Research Center for Materials and Devices''. AFL thanks the Brazilian funding agencies CAPES and CNPq for the support. RP is grateful to Dr Přemysl Kolorenč, Dr Uwe Hergenhahn, and Prof. Dr Reinhold Fink for helpful discussions.

Notes and references

1 J. McColl and F. P. Larkins, *Chem. Phys. Lett.*, 1992, **196**, 343.
2 R. Püttner, M. Domke and G. Kaindl, *Phys. Rev. A: At., Mol., Opt. Phys.*, 1998, **57**, 297.
3 T. D. Thomas, C. Miron, K. Wiesner, P. Morin, T. X. Carroll and L. J. Sæthre, *Phys. Rev. Lett.*, 2002, **89**, 223001.
4 F. Tarantelli and L. S. Cederbaum, *Phys. Rev. Lett.*, 1993, **71**, 649.
5 F. O. Gottfried, L. S. Cederbaum and F. Tarantelli, *Phys. Rev. A: At., Mol., Opt. Phys.*, 1996, **53**, 2118.
6 L. S. Cederbaum, J. Zobeley and F. Tarantelli, *Phys. Rev. Lett.*, 1997, **79**, 4778–4781.
7 J. Zobeley, R. Santra and L. S. Cederbaum, *J. Chem. Phys.*, 2001, **115**, 5076–5088.
8 U. Hergenhahn, *J. Electron Spectrosc. Relat. Phenom.*, 2011, **184**, 78–90.
9 T. Jahnke, *J. Phys. B: At., Mol. Opt. Phys.*, 2015, **48**, 082001.
10 C. Buth, R. Santra and L. S. Cederbaum, *J. Chem. Phys.*, 2003, **119**, 10575.
11 J. A. D. Matthew and Y. Komninos, *Surf. Sci.*, 1975, **53**, 716.
12 D. Céolin, J. M. Ablett, D. Prieur, T. Moreno, J. P. Rueff, T. Marchenko, L. Journel, R. Guillemin, B. Pilette, T. Marin and M. Simon, *J. Electron Spectrosc. Relat. Phenom.*, 2013, **190**, 188.
13 M. Breinig, M. H. Chen, G. E. Ice, F. Parente, B. Crasemann and G. S. Brown, *Phys. Rev. A: At., Mol., Opt. Phys.*, 1980, **22**, 520.
14 G. C. King, M. Tronc, F. H. Read and R. C. Bradford, *J. Phys. B: At. Mol. Phys.*, 1977, **10**, 2479.
15 L. Avaldi, G. Dawber, R. Camilloni, G. C. King, M. Roper, M. R. F. Siggel, G. Stefani and M. Žitnik, *J. Phys. B: At., Mol. Opt. Phys.*, 1994, **27**, 3953.
16 NIST Atomic Spectra Database, Version 5.6, https://www.nist.gov/pml/atomic-spectra-database, accessed: 2019-02-11.
17 M. Domke, R. Püttner, K. Schulz and G. Kaindl, *Phys. Rev. A: At., Mol., Opt. Phys.*, 1995, **52**, 1147.
18 R. Püttner, I. Dominguez, T. J. Morgan, C. Cisneros, R. F. Fink, E. Rotenberg, T. Warwick, M. Domke, G. Kaindl and A. S. Schlachter, *Phys. Rev. A: At., Mol., Opt. Phys.*, 1999, **59**, 3415.
19 M. O. Krause and J. H. Oliver, *J. Phys. Chem. Ref. Data*, 1979, **8**, 329.
20 K. C. Prince, M. Vondráček, J. Karvonen, M. Coreno, R. Camilloni, L. Avaldi and M. de Simone, *J. Electron Spectrosc. Relat. Phenom.*, 1999, **101–103**, 141.
21 C. Nicolas and C. Miron, *J. Electron Spectrosc. Relat. Phenom.*, 2012, **185**, 267.
22 J. N. Cutler, G. M. Bancroft, J. D. Bozek, K. H. Tan and G. J. Schrobilgen, *J. Am. Chem. Soc.*, 1991, **113**, 9125.
23 R. Püttner, M. Domke, K. Schulz and G. Kaindl, *Chem. Phys. Lett.*, 1996, **250**, 145.
24 *Structure data of free polyatomic molecules, Landolt-Börnstein, New Series, Group II*, ed. K.-H. Hellwege and A. M. Hellwege, Springer, Berlin, 1987, vol. 15, p. 96.
25 Y. Morino, K. Kuchitsu and T. Moritani, *Inorg. Chem.*, 1969, **8**, 867.
26 K. W. Hansen and L. S. Bartell, *Inorg. Chem.*, 1965, **4**, 1175.
27 P. J. Hay, *J. Chem. Phys.*, 1982, **76**, 502.
28 A. Kivimäki, J. Álvarez Ruiz, M. Coreno, M. Stankiewicz, G. Fronzoni and P. Decleva, *Chem. Phys.*, 2008, **353**, 202.
29 J. A. Bearden, *Rev. Mod. Phys.*, 1967, **39**, 78.
30 W. L. Jolly, K. D. Bomben and C. J. Eyermann, *At. Data Nucl. Data Tables*, 1984, **31**, 433.
31 J. J. Yeh and I. Lindau, *At. Data Nucl. Data Tables*, 1985, **32**, 1.
32 J. H. Scofield, *At. Data Nucl. Data Tables*, 1974, **14**, 121.
33 D. L. Walters and C. P. Bhalla, *Phys. Rev. A: At., Mol., Opt. Phys.*, 1971, **4**, 2164.
34 V. Averbukh, I. B. Müller and L. Cederbaum, *Phys. Rev. Lett.*, 2004, **93**, 263002.
35 F. Tarantelli, A. Sgamellotti and L. S. Cederbaum, *J. Chem. Phys.*, 1991, **94**, 523.
36 H. Siegbahn, L. Asplund and P. Kelfve, *Chem. Phys. Lett.*, 1975, **35**, 330.
37 S. Aksela, O.-P. Sairanen, H. Aksela, G. M. Bancroft and K. H. Tan, *Phys. Rev. A: At., Mol., Opt. Phys.*, 1988, **37**, 2934.
38 G. G. B. de Souza, P. Morin and I. Nenner, *Phys. Rev. A: At., Mol., Opt. Phys.*, 1986, **34**, 4770.
39 E. Z. Chelkowska and F. P. Larkins, *J. Phys. B: At., Mol. Opt. Phys.*, 1991, **24**, 5083.
40 F. O. Gottfried, L. S. Cederbaum and F. Tarantelli, *J. Chem. Phys.*, 1996, **104**, 9754.
41 P. Bolognesi, A. Kivimäki, P. O'Keeffe, V. Feyer, F. Tarantelli, L. Storchi and L. Avaldi, *J. Chem. Phys.*, 2011, **134**, 094308.
42 A. D. Caunt, H. Mackle and L. E. Sutton, *Trans. Faraday Soc.*, 1951, **47**, 943.
43 P. Jóvári, G. Mészáros, L. Pusztai and E. Sváb, *J. Chem. Phys.*, 2001, **114**, 8082.
44 C. F. Bunge, J. A. Barrientos and A. V. Bunge, *At. Data Nucl. Data Tables*, 1993, **53**, 113.
45 K. S. Pitzer and L. S. Bernstein, *J. Chem. Phys.*, 1975, **63**, 3849.
46 T. Åberg and G. Howat, in *Encyclopedia of Physics*, ed. S. Flügge and W. Mehlhorn, Springer, Berlin, 1982, vol. XXXI, pp. 469–619.
47 J. N. Cutler, M. G. Bancroft and K. H. Tan, *Chem. Phys.*, 1993, **181**, 461.
48 J. Palaudoux, T. Kaneyasu, L. Andric, S. Carniato, G. Gamblin, F. Penent, Y. Hikosaka, E. Shigemasa, K. Ito, S. Fritzsche, E. Kukk, S. Sheinerman, R. F. Fink, P. Lablanquie and R. Püttner, *Phys. Rev. A*, 2018, **98**, 043406.
49 T. Matila, R. Püttner, A. Kivimäki, H. Aksela and S. Aksela, *J. Phys. B: At., Mol. Opt. Phys.*, 2002, **35**, 4607.
50 E. J. McGuire, *Phys. Rev. A: At., Mol., Opt. Phys.*, 1972, **5**, 1043.

